Joint Optimization of 5.5G Cellular Networks Using Ray Tracing and PSO-MDE for Antenna Configuration and Power Allocation

Chunbing Jian¹, Fan Gong^{2*}

¹School of Communication and Information Engineering, Shanghai Technical Institute of Electronics & Information Shanghai 201411, China

²Research and Development Department, Kingsignal Technology Co., Ltd, Shenzhen 518063, China

E-mail: fangong7401@163.com

*Corresponding author

Keywords: 5.5G network, network coverage, ray tracing algorithm, PSO algorithm, pareto front

Received: April 29, 2025

In the continuous evolution of mobile communication technology, 5.5G network is a key step towards future communication, which is gradually becoming the focus of academia and industry. To solve the complex signal propagation and serious multi-path interference in high frequency band, the improved particle swarm differential evolution algorithm and multi-objective differential evolution particle swarm optimization algorithm are proposed to maximum coverage and minimum power consumption in wireless sensor networks. This method improves the efficiency of solving complex optimization problems by maintaining the global search ability and enhancing the local search performance. The experiment was carried out on a customized simulation platform and tested for different scale sensor deployment scenarios. The research results indicated that the optimal coverage after optimizing the parameters of the community antenna occurred when the inertia factor was 0.4 and 0.7, at 0.641 and 0.640, respectively. The average optimal coverage was 0.633 and 0.632 when the inertia factor was 0.6 and 0.7, respectively. The designed algorithm performed the best in reducing transmission power, computational efficiency, and exploring solution space. The minimum total transmission power reached 33.5dBm, the maximum number of Pareto front points reached 240, and the calculation time was the shortest, at 530s. The research results show that the proposed optimization algorithm can effectively improve the coverage and energy efficiency of the 5.5G network, providing an effective solution for network optimization.

Povzetek: Predstavljena je skupna optimizacija 5.5G kot RT modeliranje + PSO-MDE za azimut/nagib anten in MOPSO-DE za oddajno moč. Rezultati: večja pokritost, nižja moč, hitrejša konvergenca, več Pareto rešitev, boljša energetska učinkovitost.

1 Introduction

continuous advancement of mobile communication technology, the world is transitioning to fifth generation mobile communication technology. The 5.5G network provides strong support for emerging technologies such as the Internet of Things, augmented reality, and virtual reality with its higher data transmission rate, lower latency, and wider connectivity the high-frequency capabilities [1-2]. However, communication characteristics and ultra-dense deployment requirements of 5.5G networks also make the wireless signal propagation environment more complex, posing new challenges to network coverage and energy efficiency [3]. Traditional optimization algorithms are prone to getting stuck in local optima and have slow convergence speed under high-dimensional search spaces and nonlinear constraints, making it difficult to meet the high real-time and performance requirements of 5.5G [4]. The Ray Tracing (RT) algorithm can simulate the propagation path of electromagnetic waves, and accurately characterize the channel characteristics in high-frequency communication environments. It is suitable for 5.5G network modeling performance optimization. Particle Swarm Optimization (PSO) is a stochastic optimization method based on swarm intelligence, which has fast convergence speed and simple implementation [5-6]. The Differential Evolution (DE) strategy is a population-based stochastic optimization algorithm mainly used to solve continuous optimization problems. Therefore, the study adopts the RT algorithm for channel modeling to quantitatively evaluate network performance. An optimized PSO algorithm that combines Metropolis criterion and DE (PSO-MDE) is proposed to optimize antenna parameters. The Multi-objective PSO based on DE (MOPSO-DE) is taken to optimize the signal transmission power to improve the performance of the 5.5 network by increasing the signal propagation rate and reducing energy consumption management.

The innovation of the research lies in improving the traditional PSO algorithm, which enhances the algorithm's global search and local fine adjustment

capabilities. In addition, a crowding distance algorithm is introduced to maintain the diversity of the solution set. Compared with traditional optimization methods, the contribution of the research is to propose a joint optimization framework combining RT modeling and PSO-MDE algorithm, which can simultaneously optimize the antenna direction parameters and transmission power allocation strategy of the base station in the community. The adaptive evolution mechanism is introduced to improve the convergence speed and search accuracy in complex scenarios. Simulation experiments based on synthetic urban environment verify that the proposed method is significantly superior to the mainstream algorithm in coverage and interference control.

To systematically verify the effectiveness of the proposed method, the research aims to clearly explore whether the proposed improved algorithm is superior to the current mainstream optimization algorithm in the statistical sense in the 5.5G cellular network under the same number of nodes and deployment constraints, and evaluate its performance in energy management, especially its potential in reducing transmission power and improving energy efficiency. Therefore, two research hypotheses are proposed. One is that PSO-MDE algorithm will achieve higher network coverage than JADE and ABC algorithm. The second assumption is that PSO-MDE algorithm is better than JADE and ABC algorithm in reducing the total transmission power and energy efficiency. To verify improving assumptions, the research compares the performance of different algorithms in coverage and energy management through simulation experiments, and uses statistical methods to evaluate whether the performance improvement of PSO-MDE algorithm is statistically significant.

The research will be divided into the following five sections. Section 1 introduces the relevant background and existing research. Section 2 describes the proposed joint optimization method. Section 3 presents the experimental results and performance analysis. Section 4 discusses the results and compares them with recent studies. Section 5 summarizes the full text and looks forward to future work.

2 Related works

The rapid development of wireless communication technology has made network performance optimization increasingly important. Mao et al. proposed a damage assessment method based on convolutional neural networks from components to the overall structure to address the post-earthquake damage assessment needs of reinforced concrete communication buildings. The research results indicated that the proposed method was highly consistent with the expert evaluation conclusions, and the optimized convolutional neural network had good accuracy and stability [7]. Yu et al. proposed a system optimization method based on Reconfigurable Intelligent Surfaces (RIS) to achieve ultra-wireless bandwidth, ultra large-scale connectivity, and highly

reliable communication in 6G communication networks. By reviewing relevant research literature in recent years, the performance optimization of RIS assisted wireless communication networks was summarized and the potential future research direction for RIS assisted communication network deployment was explored [8]. Liang et al. proposed a traffic control scheduling generation method for train communication networks based on improved incremental scheduling strategy and improved grey wolf optimization algorithm to meet the high transmission demand of massive real-time data in intelligent rail transit. The research results indicated that this method had advantages in computational accuracy and speed, and could reduce the average end-to-end delay to 57 µs [9]. Yu et al. proposed a joint cross-layer optimization framework to address the deep learning semantic encoding and decoding exacerbating traditional communication energy consumption. The research results indicated that the framework could effectively solve the joint optimization problem of semantic and physical layers by jointly optimizing physical layer power control and semantic layer compression allocation [10].

Network optimization often involves multiple objectives, such as coverage, capacity, energy efficiency, and cost. The PSO algorithm, especially its multiobjective version, can effectively handle these multiobjective optimization problems and find the optimal solution that balances different objectives. Hu et al. proposed an intelligent deployment method for emergency ground to air communication networks based on a hybrid layered PSO algorithm to effectively respond to the transmission of emergency monitoring data during large-scale environmental emergencies. The research results indicated that this method could adaptively update the deployment location and communication link of emergency communication resources, significantly improve adaptability after multiple iterations, and achieve comprehensive coverage and distribution of communication nodes [11]. Wang et al. proposed a multi-objective PSO algorithm to solve the time-consuming and inefficient design of traditional terahertz metamaterial absorbers. The research results indicated that this method could achieve dual objective optimization of absorber structural parameters with absorption rate and quality factor as independent objectives, significantly improving design efficiency and performance [12]. Nuthakki et al. proposed an AI driven method using an improved multi-objective PSO algorithm to achieve high resource utilization in cloud data centers in intelligent manufacturing environments. The research results indicated that this method outperformed other multi-objective algorithms in allocation intelligent optimizing resource in manufacturing cloud environments [13].

To sum up, the existing methods may perform well in specific environments, but the generalization ability and adaptability need to be improved, and some algorithms have high computational complexity. The trade-offs and balances between different objectives still need to be further analyzed. Table 1 compares the

application environment, key results, research gaps, and SOTA drawbacks of each network optimization method. Therefore, the research combines RT algorithm to optimize the 5.5G network, and introduces de-mutation and crossover operation to improve the traditional PSO

algorithm, aiming to improve the adaptability, real-time performance and optimization efficiency of the algorithm, so as to better meet the challenges of network optimization in large-scale and complex environments.

Table 1: Comparison of research results of various network optimization methods.

Reference	Algorithm	Application environment	Key results	Limitations of SOTA		
[7] Mao C X et al.	Convolutional neural network	Post-earthquake damage evaluation of RC frame communication buildings	High consistency with expert assessment; optimized CNN model shows good accuracy and stability	Lack of verification of algorithm generalization capability		
[8] Yu W W et al.	RIS auxiliary network optimization	6G communication networks Enhances communication performance		High computational complexity; lacks real-time capability		
[9] Liang C et al.	Improved grey wolf optimization algorithm	Train communication networks in intelligent rail transit	Reduces average end-to-end latency to $57\mu s$	Algorithm adaptability needs improvement		
[10] Yu K W et al.	Joint cross-layer optimization framework	Communication energy consumption in deep learning semantic encoding and decoding	Effectively addresses the joint optimization issue of semantic and physical layers	Further research focuses on trade-offs between different objectives		
[11] Hu W Z et al.	Hybrid hierarchical PSO algorithm	Intelligent deployment of emergency aerial-ground communication networks under large-scale sudden environmental events	Significantly improves fitness after multiple iterations; achieves comprehensive coverage and balanced distribution of communication nodes	Performs well in specific environments but lacks generalization capability		
[12] Wang Y R et al.	MPSO	Design of terahertz metamaterial absorbers	Achieves dual-objective optimization of absorber structure parameters, significantly improving design efficiency and performance	Lacks universal solutions for broader scenarios		
[13] Nuthakki P et al.	Improved MPSO	Resource allocation in cloud data centers for smart manufacturing	Outperforms other multi-objective algorithms in optimizing resource allocation in smart manufacturing cloud environments	The computational complexity and real-time capability of the algorithm need further optimization		

3 Methods and materials

Optimization of antenna parameters for 5.5G network in community based on RT and improved PSO-MDE algorithm

Signal propagation and energy management are two key dimensions in 5.5G network optimization. Signal propagation can improve signal coverage quality and reduce interference by optimizing antenna parameters, while energy management can reduce energy consumption by optimizing transmission power [14-15]. Therefore, a sequential linkage two-stage optimization framework is proposed to improve the configuration efficiency of antenna parameters and transmission power in 5.5G cellular network. In this framework, PSO-MDE is first used to optimize the antenna azimuth and tilt angle of each sector to maximize the signal coverage in the cell. Then, taking the obtained antenna parameters as input, MOPSO-DE is used to further optimize the transmission power of each sector, while considering minimizing power overhead and maximizing overall coverage. This two-stage strategy decouples the complex search space and avoids the convergence difficulty in high-dimensional joint optimization. The dependent path is clear, and the subsequent power optimization stage is directly affected by the antenna parameters in the early stage. It also has strong scalability. Firstly, a cellular network structure is constructed to visually demonstrate the spatial layout relationship between typical cell division and base station antennas. The cellular network structure is shown in Figure 1.

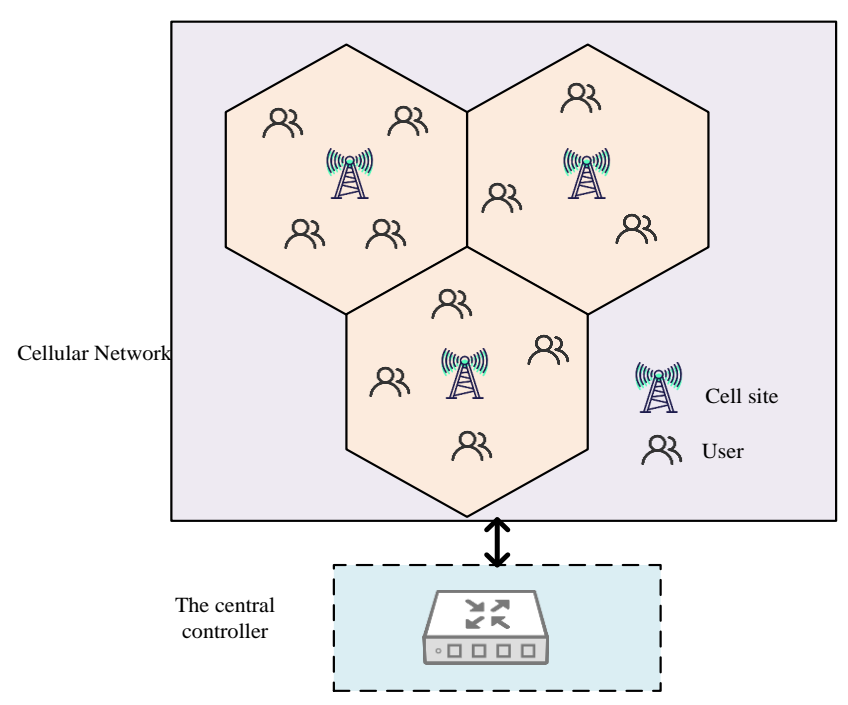


Figure 1: Schematic diagram of cellular network structure and base station layout.

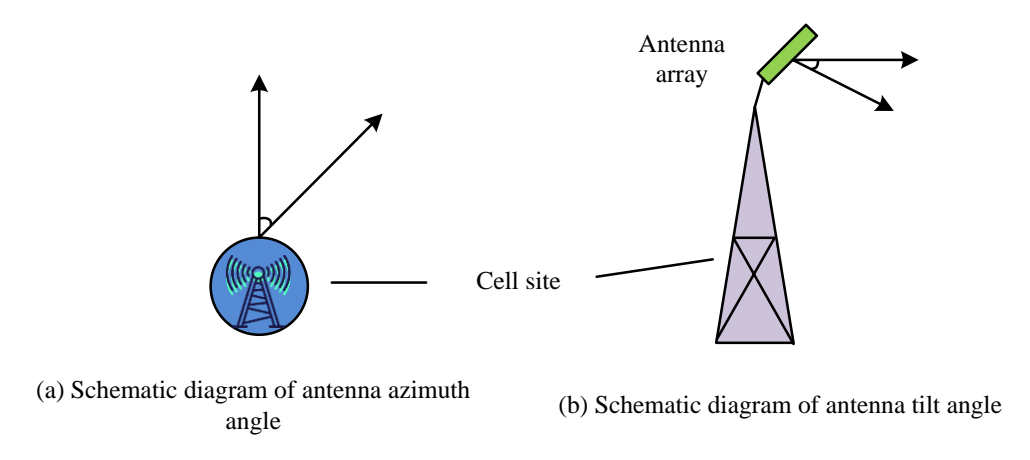


Figure 2: Schematic diagram of antenna azimuth angle and tilt angle.

As shown in Figure 1, a cellular network consists of multiple base stations, each responsible for covering one or more sectors, forming a hexagonal structure similar to a honeycomb. Each antenna of the three-sector base station is responsible for covering an area within 120°, and the antenna can independently set its direction and tilt angle. In this structure, antenna parameters directly determine the direction and intensity distribution of signal radiation. Reasonable configuration effectively expand the effective coverage area, and reduce blind spots and overlapping interference [16]. In this cellular structure, each sector is considered as an independent optimization unit, and the antenna parameters of all 21 sectors are jointly optimized. Therefore, the optimization problem has a highdimensional search space with 42-dimensional continuous variables. The optimization goal is to maximize the overall coverage performance and signal power distribution quality in the region by adjusting the antenna azimuth and tilt angle of all sectors under the fixed network topology and deployment architecture. This study refers to the areas where communities serve each department, rather than macro level residential areas. The designed dual-objective fitness function is based on the proportion of users who meet the signal strength threshold (coverage) and the average received power level in the whole simulation area. To ensure the authenticity and challenge of the modeling, this study did make assumptions about simplifying sector deployment strategies, nor did it incorporate sector or shared antenna parameters. However, it retains a completely independent antenna configuration, making the optimization task closer to the requirements of real cellular network configuration. The azimuth and tilt angle parameters of the antenna are two key control

parameters for the community antenna, as shown in Figure 2.

As shown in Figure 2, the horizontal direction of the main beam of the azimuth antenna controls the angle range of signal coverage, usually from 0° to 360°. The vertical pitch angle of the tilt angle controls the degree of tilt of the main lobe of the signal, usually set between 0° and 15°. If the beam is too small, it will move towards the far end, which may cause cross zone interference. If it is too large, the signal will be concentrated in the near end, resulting in poor reception for remote users [17]. In the 5.5G high-frequency communication environment, to more accurately capture the propagation path and loss law of signals in complex environments, the RT algorithm is used for channel modeling to quantitatively evaluate the coverage performance of cellular networks. The RT method accurately models the signal propagation characteristics by simulating the reflection, diffraction, and penetration paths of radio waves in real environments. The total channel loss is shown in equation (1).

$$L(d) = L_0 + 10n \log_{10}(d) + \sum_{i=1}^{M} L_{ij}$$
 (1)

In equation (1), L_0 represents the free space path loss. n represents the path loss index, which is set according to specific scenarios. S represents the transmission distance. L_{rj} represents the additional loss caused by the j-th reflection or diffraction. Mrepresents the total number of multi-path components. The antenna parameter optimization is to maximize the coverage within the area. The received power at each user's location is shown in equation (2).

$$P_{r,i} = P_t + G(\theta_i, \phi_i) - L(d_i)$$
 (2)

In equation (2), $P_{r,i}$ is the received power of the i-th receiving point. P_t is the power of the transmitted signal. $G(\theta_i, \phi_i)$ represents the gain function. θ_i represents the angle with the receiving point. ϕ_i represents the relevant antenna gain. $L(d_i)$ is the path loss. The grid-based evaluation method can divide the research area into several equally spaced small grids, calculate and statistically analyze the received signal strength of each grid point, and evaluate the overall coverage performance. Coverage refers to the proportion of areas in which the received signal strength indicator (RSSI) exceeds a preset threshold in a specific area. It reflects

the signal coverage quality of the network in the region. To accurately evaluate the coverage, the RSSI threshold and analysis window are defined. The RSSI threshold is set to -90dbm. Only when the RSSI value is higher than this threshold, the area is considered to be effectively covered. The analysis window is defined as a meshed area, and each grid point represents a measurement point. The coverage is determined by calculating the RSSI value of each grid point and determining whether it exceeds the threshold. It is commonly used for signal coverage analysis and optimization in wireless networks. The coverage rate of the community is shown in equation

$$\eta_{\text{cov}} = \frac{\sum_{i=1}^{N} \mathcal{S}(P_{r,i} \ge P_{\text{th}})}{N}$$
 (3)

In equation (3), η_{cov} is the coverage probability, representing the probability that the received power is greater than a certain threshold P_{th} . δ is an indicator function ranging from 0 to 1. N is the total number of grids. This method can accurately evaluate the coverage performance of the network and use it as the objective function for optimization. Further research will encode the antenna azimuth and tilt angle of each community as variables to form a "particle" in the particle swarm. Taking the total coverage within the region as the fitness function, the optimal combination of antenna parameters is obtained. The optimization objective function for maximizing coverage is shown in equation (4).

$$F = \max_{\phi_i, \theta_i} \eta_{cov}(\phi_i, \theta_i)$$
 (4)

In equation (4), F is the optimized objective function. (ϕ_i, θ_i) represents the azimuth and elevation angles of the i -th receiving point. The parameter modeling is completed. Coverage optimization has nonlinear and multi peak characteristics, while PSO still suffers from premature convergence in high-dimensional complex spaces. Therefore, the DE is introduced to improve the PSO algorithm. DE can generate new solutions by mutating and recombining individual differences, and has strong global search capabilities. In addition, the research also introduces the Metropolis criterion and adaptive inertia factor to enhance the ability to escape from local optima, balancing global exploration and local development. The specific process of PSO-MDE algorithm is shown in Figure 3.

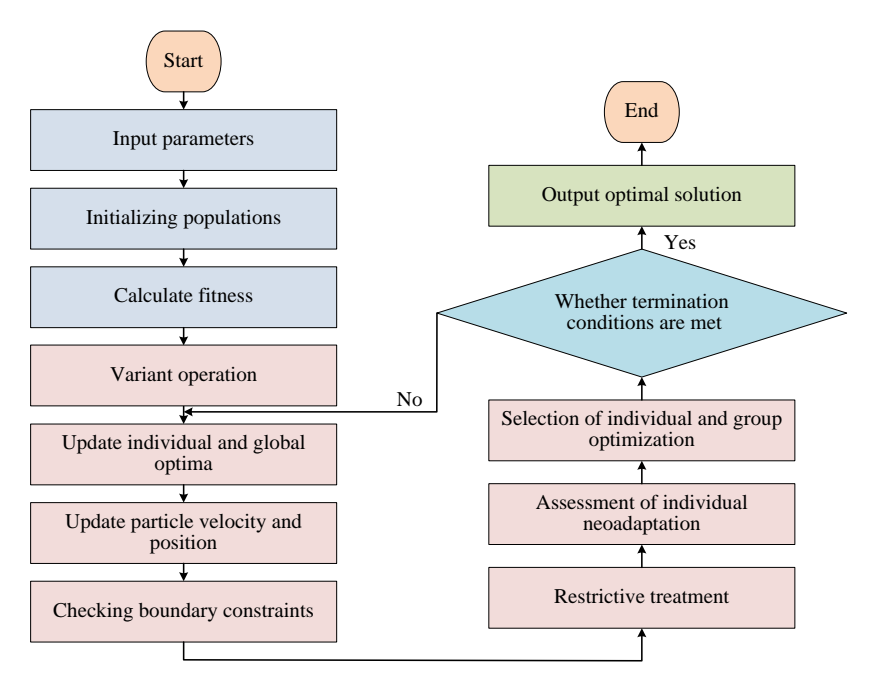


Figure 3: Flow chart of PSO-MDE algorithm.

From Figure 3, firstly, the position, velocity, and fitness values of the particle swarm are initialized, and the inertia factor is set. In each iteration, particles move according to velocity and position update equations. The adaptive inertia factor dynamically adjusts according to the iteration process to achieve a balance from global search to local fine search. The particle velocity and position updates combine the velocity update mechanism of PSO with the mutation crossover operation of DE. Specifically, the velocity update of particles follows the velocity update equation of the standard particle swarm algorithm, and introduces adaptive inertia weights to dynamically adjust the motion trend of particles. This process ensures that particles can search effectively according to the individual optimal position and the global optimal position. The variant operation is part of the PSO update cycle and directly participates in updating particle positions rather than being independent of the main cycle. The specific calculation is shown in equation (5).

$$\omega = \omega_{\min} + (\omega_{\max} - \omega_{\min}) \exp\left(-\lambda \left(\frac{k}{k_{\max}}\right)\right)$$
 (5)

In equation (5), ω is the current inertia factor. k is the number of iterations. λ is a parameter that controls the inertia factor to reduce speed. In the location update phase, mutation and crossover operations of DE are

introduced to enhance the diversity and global search ability of the population. Specifically, for each particle, firstly, the mutation operation of DE is performed, selecting three different particles and calculating their difference vectors, and then adding them to the current position of the particles to generate a new mutation vector. Then, the DE crossover operation is performed, and some components of the mutation vector are replaced with a certain probability at the current particle position to generate a test vector. This test vector is then used to evaluate its fitness. If the fitness is better than the current particle position, the particle position is updated. In this way, DE mutation and crossover operation provide new candidate solutions for PSO and increase the diversity of the population. In this way, PSO-MDE combines the fast convergence characteristics of PSO and the global search ability of DE to improve the optimization performance. If the newly generated particles are better than the current solution, they will be updated directly. If it is inferior to the current solution, it is accepted with a certain probability according to the Metropolis criterion to avoid falling into local optima. During the iteration process, the individual extremum and global optimal solution are continuously updated until the termination condition is met. The pseudo-code of PSO-MDE algorithm is shown in Figure 4.

```
// Initialize parameters
Set population size N, maximum number of iterations T, inertia weight ω, cognitive component c1,
social component c2
Set differential evolution scaling factor \lambda, crossover probability CR
// Initialize the swarm
For i = 1 to N:
  Randomly initialize particle position position[i] and velocity velocity[i]
  Evaluate fitness fitness[i]
  If fitness[i] is better than personal best pbest[i]:
     Update pbest[i] = position[i]
  If fitness[i] is better than global best gbest:
     Update gbest = position[i]
// Start iterations
For t = 1 to T:
  For i = 1 to N:
     // Differential Evolution Mutation
     Randomly select j, k, 1 \neq i from \{1, 2, ..., N\}
     Calculate mutation vector mutant = pbest[i] + \lambda * (position[j] - position[k]) + (position[l] -
position[j])
     // Differential Evolution Crossover
     Create trial vector trial = position[i]
     For each dimension d = 1 to D:
        If rand() < CR or d = randomly chosen dimension:
          Set trial[d] = mutant[d]
     // Evaluate trial vector fitness fitness[trial]
     If fitness[trial] is better than fitness[i]:
        Update position[i] = trial
     // PSO velocity and position update
     Update velocity[i] = \omega * velocity[i] + c1 * rand() * (pbest[i] - position[i]) + c2 * rand() * (gbest
position[i])
     Update position[i] = position[i] + velocity[i]
  // Update global best
  For i = 1 to N:
     If fitness[i] is better than gbest:
        Update gbest = position[i]
// Output results
Return global best solution gbest
```

Figure 4: Pseudo-code of PSO-MDE algorithm.

From Figure 4, in pseudo-code, key symbol or variable mutation represents mutation operation, crossover represents crossover operation, and CR represents crossover probability in DE. PSO-MDE algorithm combines the advantages of PSO and DE, and enhances the global search ability of PSO by introducing DE mutation and crossover operation. In the initialization phase of the algorithm, the position and speed of the particle swarm are randomly generated, and the fitness is evaluated. In the iteration process, the DE strategy is used to update the particle velocity, and the parameters

such as mutation factor and crossover probability are automatically adjusted to meet the needs of different search stages. This improved strategy helps the particles jump out of the local optimum, improves the diversity of solutions, and speeds up the convergence speed. Finally, PSO-MDE algorithm shows better performance in multi-objective optimization problems and has wide application potential.

3.2 Power allocation optimization based on MOPSO-DE

To ensure the feasibility and robustness of the optimization process, the series optimization architecture is adopted. In phase 1, the fixed initial transmission power is analyzed, and the antenna azimuth and tilt angle of the sector are optimized by PSO-MDE. On this basis, in phase 2, MOPSO-DE is used to further refine and optimize the transmission power of each sector. The output of antenna angle is directly used as the input environment variable in the power optimization phase rather than sharing variable parameters to ensure the consistency of physical configuration. Next, the study optimizes the energy consumption of the 5.5G network. Due to the uneven spatial distribution of business demands in complex urban environments, it is necessary to allocate transmission power reasonably to ensure network coverage and energy efficiency. Therefore, the study selects maximum coverage and minimum total transmission power as optimization objectives to construct a multi-objective optimization model [18-19]. MOPSO has good global search capability when dealing with multi-objective problems. However, it has shortcomings in maintaining population diversity and improving local accuracy [20]. Therefore, to optimize the signal transmission power in residential areas, the research has also adopted DE to improve MOPSO. The MOPSO-DE process is shown in Figure 5.

From Figure 5, first, the individual particle swarm is initialized. Each particle represents a cell transmission

power combination. The initialization process includes initializing the position and speed of the particle swarm. The initial position of each particle is set to its initial personal optimal value. In this way, the algorithm can provide a reasonable starting point for each particle in the initial stage, so as to improve the optimization efficiency. Secondly, the fitness of individuals under the two objectives of "maximizing regional coverage" "minimizing total transmission power" is calculated through the objective function. All non-dominated solutions will enter the external elite pool and use crowding distance sorting to maintain the diversity of the solution set. During the iteration process, particles update by guiding individuals to learn the historical optimal position and performing differential mutation operations. The updated velocity is shown in equation (6).

$$v_e = x_{r1} + u \cdot (x_{r2} - x_{r3}) \tag{6}$$

In equation (6), v_e is the variation vector of the e-th particle. x_{r1} , x_{r2} , and x_{r3} are the current position vectors of three different particles randomly selected from the current population. u is the differential variation scaling factor. The specific calculation of its position is shown in equation (7).

$$x_e^{t+1} = x_e^t + v_e (7)$$

In equation (7), x_e^{t+1} and x_e^t are the current position vectors of the e-th particle in the t+1-th and t-th generations, respectively. v_e is the velocity vector obtained through differential variation. The pseudo-code of MOPSO-DE algorithm is shown in Figure 6.

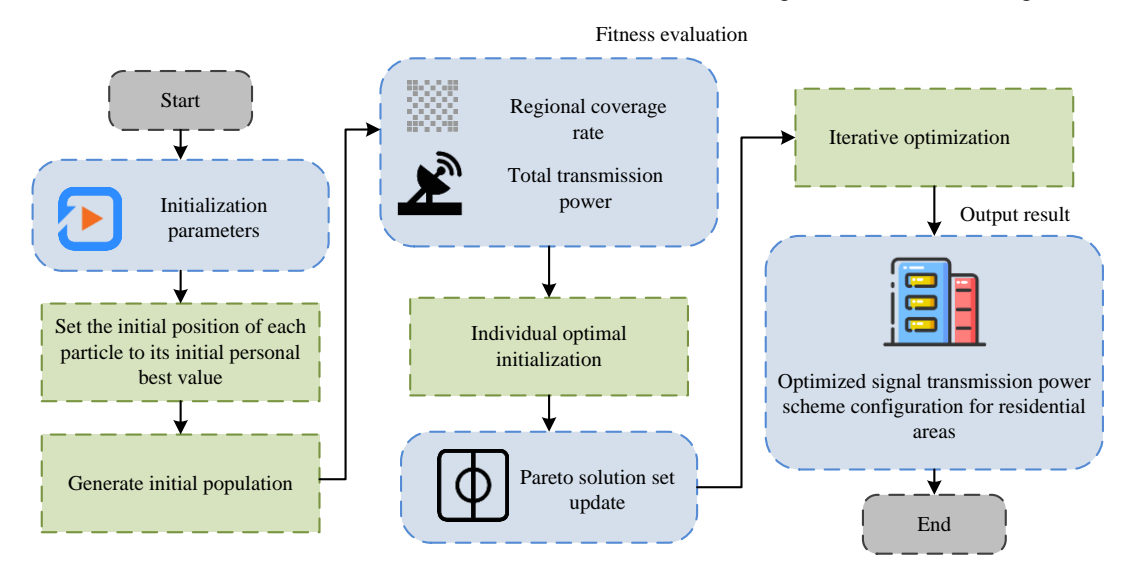


Figure 5: Optimization of signal transmission power in community based on MOPSO-DE algorithm.

```
// Initialize the parameters
Set the number of particles N, maximum iterations T, mutation factor F, crossover probability CR
Initialize the position and velocity of each particle randomly
// Initialize the archive with the initial particles
for each particle i from 1 to N do
  Evaluate the fitness of particle i
  if particle i is non-dominated then
     Add particle i to the archive
  end if
end for
// Main loop
for iteration from 1 to T do
  for each particle i from 1 to N do
    // Differential Evolution Mutation
    Choose three distinct particles j,\,k,\,l different from i
     V = particle[j] + F * (particle[k] - particle[l])
    // Differential Evolution Crossover
     U = particle[i]
     for each dimension d from 1 to D do
       if rand() < CR or d is a random dimension then
          U[d] = V[d]
       end if
     end for
    // Evaluate the fitness of the trial vector U
    Evaluate the fitness of U
    // Non-dominated sorting
    if U dominates particle[i] then
       Replace particle[i] with U
     else if U is non-dominated and dominates some particles in the archive then
       Replace the dominated particles in the archive with U
    // Update the personal best position of particle i if necessary
    if U is better than the personal best of particle i then
       Update the personal best of particle i
     end if
  end for
  // Update the global best position if necessary
  Update the global best position from the archive
end for
// Output the Pareto front
Return the archive as the Pareto front
```

Figure 6: Pseudo-code of MOPSO-DE algorithm.

From Figure 6, the pseudo-code of MOPSO-DE algorithm integrates PSO and DE for multi-objective optimization. The key parameters include the number of particles, the number of iterations, and the variation factor F. The particle position is randomly initialized, a new solution is generated through DE, and the non-dominated archive is evaluated and updated. The individual and global optima are updated iteratively. Finally, the Pareto front solution set is obtained.

Subsequently, based on the Pareto dominance relationship and crowding distance, individual strengths and weaknesses are judged, and the elite pool is updated. The Pareto optimal solution set is an ideal state of resource allocation in multi-objective optimization. All these sets of non-dominated solutions form the Pareto front in the objective space. The Pareto front diagram is shown in Figure 7.

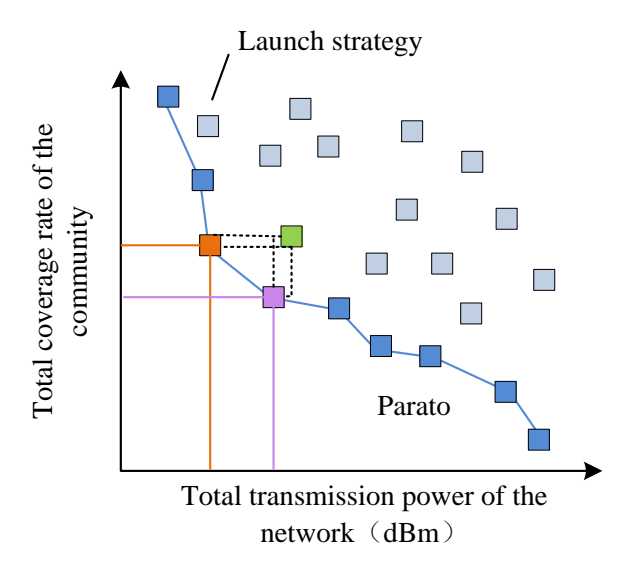


Figure 7: Pareto front diagram for multi-objective optimization.

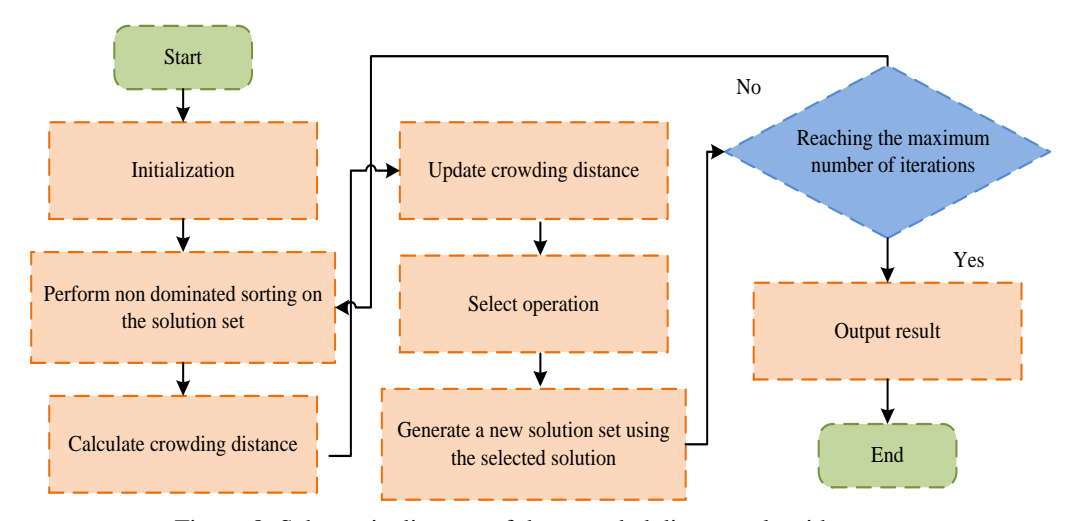


Figure 8: Schematic diagram of the crowded distance algorithm.

Figure 7 shows the Pareto front of the multiobjective optimization problem, which is used to show the dual-objective optimization relationship between coverage and transmission power, as well as the corresponding mechanism between the "Pareto front" and the actual deployment strategy. It does not correspond to specific experimental data. The graph covers the nondominated solutions in several experiments. Pareto front represents the solution set that achieves the optimal balance among multiple objectives. The horizontal axis in the figure represents the total transmission power of the network, measured in DBM, while the vertical axis represents the total coverage area of the cell. Each point corresponds to a launch strategy that meets the constraints. Due to the natural conflict between the two objectives, the optimal solution cannot be achieved simultaneously. Therefore, the output solution of this algorithm is not the only optimal solution, but rather constitutes an optimal set, namely the Pareto front. Decision makers can select appropriate equilibrium points in the Pareto front based on the needs of different

business scenarios. The mathematical definition of Pareto solution is shown in equation (8).

$$\begin{cases} \text{Maximize } f_1(x) = A(x) \\ \text{Minimize } f_2(x) = \sum_{i=1}^{N} P_i \end{cases}$$
 (8)

In equation (8), $f_1(x)$ is the sum of the total coverage rate of the community and the coverage rate A. $f_2(x)$ is the total transmission power. x is a set of parameters that includes the transmission power of each base station. P_i is the transmission power of the i-th base station. After sorting the non-dominated solutions, to prevent the solution set from being too concentrated on the Pareto front, the crowding distance algorithm is introduced as an auxiliary evaluation metric to maintain the diversity of the solution set. Crowding distance measures the distance between an individual and other non-dominated solutions in the solution space. A higher value indicates that the area in which the individual is located is sparser and more representative. The specific calculation process is shown in Figure 8.

As shown in Figure 8, firstly, all non-dominated solutions are sorted in ascending order according to their respective objective functions. Secondly, the maximum and minimum crowding distances of individuals in each target dimension are set to infinity to preserve the boundary solutions. Subsequently, the difference between each remaining solution and adjacent solutions in each target dimension is calculated and normalized. Finally, the normalized distances on all target dimensions are accumulated to obtain the total crowding distance of the solution. A large crowding distance indicates that the solution is located in a sparser area, and priority should be given to preserving it to enhance the diversity of the population. This mechanism effectively avoids the aggregation of individuals in the solution set and helps generate a wider and more evenly distributed Pareto front. Crowding distance measures the density of solutions around a solution in the objective function space. The solution with larger crowding distance means that it is relatively isolated in the target space, that is, there are fewer solutions around, which helps to maintain the diversity of solution set. To calculate the crowding distance, the non-dominated solutions are sorted for each objective function, and then the infinite crowding distance is assigned to the boundary solution. The distance difference between each solution and adjacent solutions in each target dimension is calculated and normalized. Finally, the normalized distances of all target dimensions are accumulated to obtain the total crowding distance of each solution, which is used to evaluate the diversity of solutions. The specific calculation is shown in equation (9).

$$D_{i}^{m} = \frac{f_{m}(i+1) - f_{m}(i-1)}{f_{m}^{\max} - f_{m}^{\min}}$$
(9)

In equation (9), D_i^m represents the rate of change or difference of the i-th data point in the m-th dimension. $f_m(i+1)$ and $f_m(i-1)$ are the function values of the direct successor and direct precursor of the ith solution on the m-th objective function, respectively. f_m^{\max} and f_m^{\min} are the maximum and minimum values of all solutions on the m-th objective function, respectively. The total crowding distance is the sum of the dimensions of each target, as shown in equation (10).

$$D_{i} = \sum_{m=1}^{M} D_{i}^{m} \tag{10}$$

In equation (10), M is the total number of dimensions. D_i is the comprehensive rate of change or difference of the i-th data point across all dimensions. Crowded distance contributes to the convergence and diversity of equilibrium solutions in multi-objective optimization processes. For example, three solutions are considered, including A (0.8, 0.2), B (0.9, 0.5), and C (0.95, 0.7) in the dual-objective problem. After the targets are arranged in ascending order, B is between A and C. The crowded distance is combined with the distance between the left and right solutions of B in each target dimension to calculate the sparsity of its local solution. If the solution around solution B is sparse and

the crowding distance is large, it is more likely to be retained in the next generation. Throughout the process, the MOPSO-DE algorithm approaches the Pareto optimal solution set through continuous iterations, achieving intelligent scheduling and optimized allocation of signal transmission power [21-22]. In the 5.5G network optimization, energy efficiency is a key performance index, which measures the energy efficiency of the network when transmitting data. The calculation is shown in equation (11).

$$\eta_E = \frac{T}{E} \tag{11}$$

In equation (11), η_E is energy efficiency. T is the network throughput. E is the total energy consumption. Improving energy efficiency directly means reducing energy consumption without sacrificing network throughput. By optimizing the network configuration, adjusting the antenna parameters, reducing the transmission power, and other measures, the network energy consumption can be significantly reduced and the network throughput is improved while maintaining the network performance. The antenna parameters are optimized. By adjusting the azimuth and dip angle of the antenna and optimizing the signal coverage, unnecessary energy consumption can be reduced. The transmission power is reduced. By optimizing signal transmission strategies, the transmission power of base stations can be reduced while maintaining network coverage and Using energy-saving equipment selecting network devices with energy-saving functions, such as routers and switches, can effectively reduce energy consumption. Intelligent energy management is adopted to dynamically adjust the energy consumption of equipment according to the network load to achieve the energy saving goal. The combination of these optimization strategies and MOPSO-DE algorithm is conducive to the intelligent scheduling and optimal allocation of signal transmission power [23-24].

4 Results

4.1 Experimental environment and data sources

The algorithm models and simulation programs used in the research are developed and run in the Windows 11 operating system environment. The programming language used is Python 3.10, mainly relying on scientific computing and drawing libraries such as NumPy, Matplotlib, SciPy, etc. The computing platform is an Intel Core i7-12700H processor with 16GB of memory. The topology structure of the residential area used in the simulation refers to typical urban residential scenarios. The simulation area is divided into a square area of 100m×100m, containing 7 cellular base stations, deployed with three sector antennas. The simulation area size represents a typical urban macro cellular cell. It can capture the key features of signal propagation in urban environments, such as building occlusion, street layout,

Parameter categories	Parameter name	Parame ter values	Paramet er categories	Parameter name	Parameter values	
	Number of base stations	1 10 1		Ray tracing model	Including reflection, diffraction and penetration	
	Number of sectors	30		Path loss index	2.5-3.5	
Network	Frequency band	26 GHz	Channel	Total number of multipath components	10	
configuration	Bandwidth	100 MHz	model	Terrain attenuation factor	0.5-1.5	
	Power emission range	20-40 dBm		Building penetration loss	10-20 dB	
	Receive signal strength threshold	-90 dBm		1	\	

Table 2: Experimental environment parameters.

and multi-path effects, without requiring excessive computational complexity. Urban macro cellular cells usually cover hundreds of meters, so a 100×100 meter area can well simulate this environment. In addition, this size includes sufficient buildings and obstacles in the simulation to reflect the complexity of signal propagation in urban environments. The number of particles is set to 50 to balance the search ability and computational efficiency. The convergence criterion is that the maximum iteration is 500 times or the change of fitness function value is less than 0.001. The experiment runs 30 times to evaluate the stability of the algorithm. The random seed is fixed at 42 to ensure that the experiment can be repeated. The reflection coefficient of RT simulation configuration is set to 0.6 to simulate the typical reflection behavior in urban environments. The path loss index is set between 2.5 and 3.5 to simulate signal attenuation in different environments. In addition, the terrain attenuation factor is considered to be within 0.5 to 1.5 and the building penetration loss is set between 10 and 20 dB. The network configuration and channel model parameters for the experiment are shown in Table 2.

4.2 Performance analysis of community antenna parameter optimization algorithm based on PSO-MDE

In the optimized cellular network community antenna parameters based on PSO-MDE algorithm, to comprehensively evaluate the performance of PSO-MDE algorithm, new optimization algorithms such as Artificial Bee Colony (ABC) and Adaptive Differential Evolution

Algorithm (JADE) are introduced for comparative experiments. The adaptive inertia factor can be dynamically adjusted based on the information obtained during the search process. Therefore, this study explores the influence of inertia factors on the optimization effect of parameters, and the results are shown in Figure 9.

Figure 9 (a) shows the influence of inertia factor control parameters on optimization performance. Figure 9 (b) shows the comparison results of standard deviations for different algorithms. According to Figure 9 (a), as the inertia factor increased from 0 to 1, the coverage showed a fluctuating trend. The optimal coverage occurred when the inertia factor was 0.4 and 0.7, reaching 0.641 and 0.640, respectively. The average optimal coverage was 0.633 and 0.632 when the inertia factor was 0.6 and 0.7, respectively. As shown in Figure 9 (b), the standard deviation of the PSO-MDE algorithm was always the lowest, about 1.3×10-3, indicating its good stability under different inertia factors. The standard deviations of ABC and JADE algorithms were relatively high, ranging from approximately 1.4×10 -3to 1.5×10 -3and 1.5×10 -3 to 1.6×10-3, respectively, with significant fluctuations. This may be because the PSO-MDE algorithm has advantages in parameter adjustment and adaptability, allowing it to maintain good stability and consistency under different conditions. Based on the convergence speed and optimization effect, the algorithm iteration was carried out when inertia factor influencing parameter was 0.3. To comprehensively evaluate the proposed algorithm, a comparative experiment was conducted on the coverage optimization of the three algorithms, with 20 repetitions. The obtained results are shown in Figure 10.

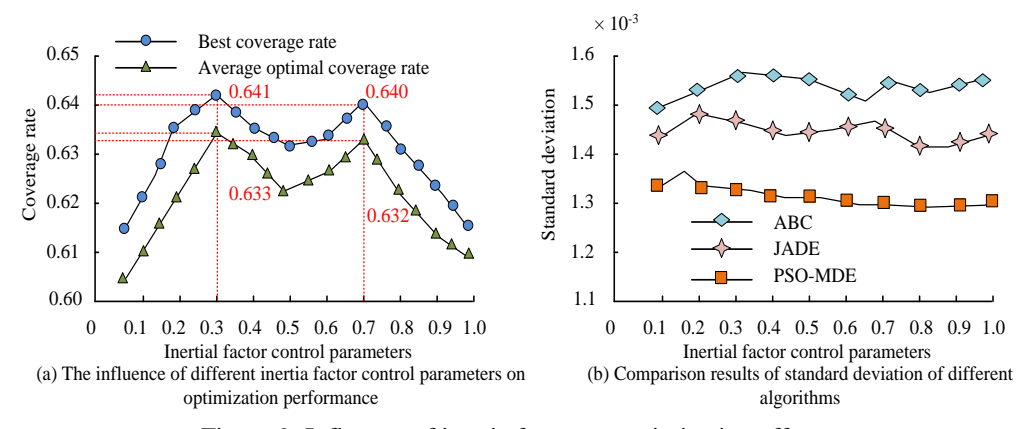


Figure 9: Influence of inertia factor on optimization effect.

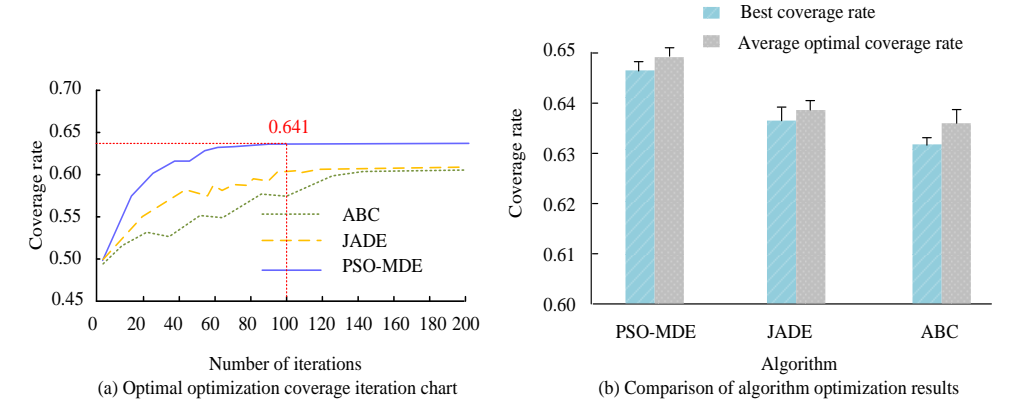


Figure 10: Comparison of coverage of different algorithms.

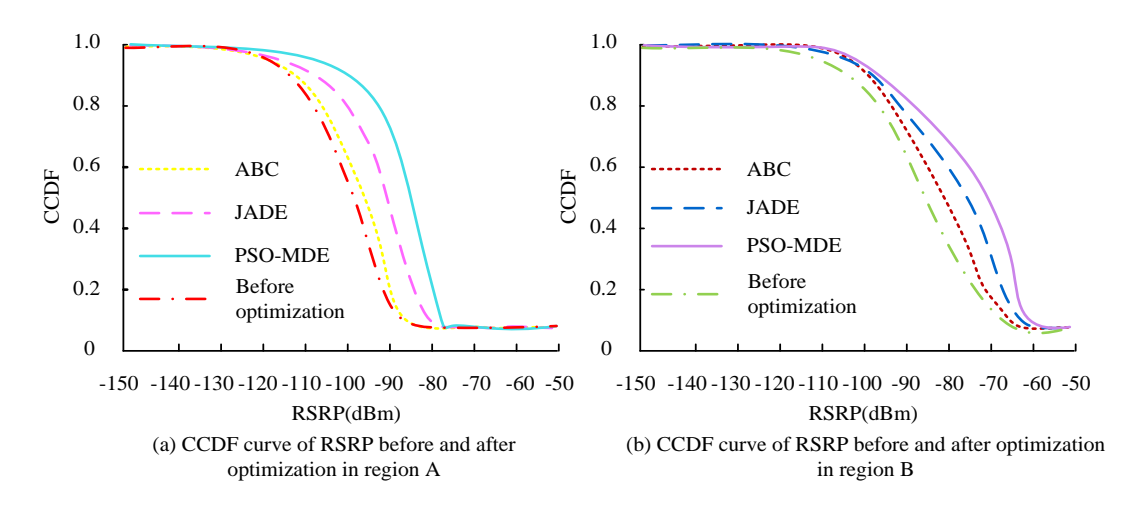


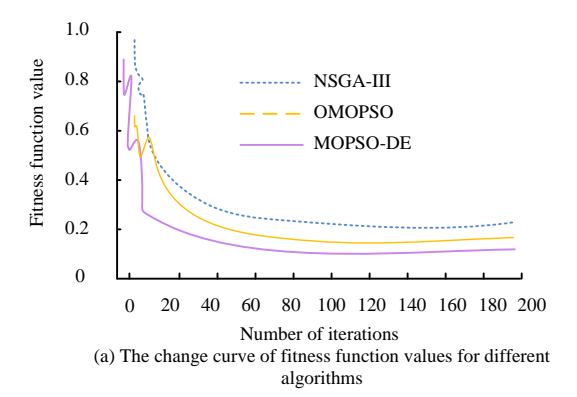
Figure 11: Comparison results of CCDF of different algorithms.

Figure 10 (a) shows the iterative variation of optimal coverage for different algorithms. Figure 10 (b) compares coverage optimization results of different algorithms on the target area. As shown in Figure 10 (a), the PSO-MDE algorithm quickly converged after about 100 iterations, and the final coverage rate reached about 0.641. After 120 and 140 iterations, JADE and ABC achieved optimal coverage rates of approximately 0.602 and 0.559, respectively. According to Figure 10 (b), PSO-MDE led in both the optimal coverage and average optimal coverage indicators, with values of

approximately 0.645 and 0.648, respectively. The optimal coverage and average optimal coverage of JADE and ABC were approximately 0.637 and 0.639, as well as 0.633 and 0.635, respectively. The reason for this result is that although JADE improves the adaptability of traditional DE, there may still be problems with slow convergence speed or falling into local optima in multidimensional search spaces. The ABC algorithm has relatively weak exploration ability due to its dependence on the honey source update mechanism. To verify the optimization effect of the algorithm on different regions,

two publicly available urban residential regions A and B are selected for comparative experiments on their grid Reference Signal Received Power (RSRP). The Complementary Cumulative Distribution Function (CCDF) is taken to evaluate the coverage quality of the network. The obtained results are shown in Figure 11.

Figures 11 (a) and (b) show the CCDF curves of regions A and B before and after optimization, respectively. As shown in Figure 11 (a), after optimizing region A, the CCDF curves of all algorithms shifted to the right, indicating an overall improvement in RSRP values and signal quality. The CCDF curve optimized by PSO-MDE algorithm was the closest to the right, indicating its optimal performance in improving RSRP. When the CCDF was 0.8, the RSRP value of PSO-MDE was about -85dBm, while ABC and JADE were about -95dBm and -90dBm, respectively. This is because PSO-MDE has better adaptability and search ability when dealing with multi-objective optimization problems. From Figure 11 (b), in region B, the CCDF curves of all optimized algorithms were significantly better than before optimization, indicating the positive effect of the optimization on improving RSRP. Specifically, the PSO-MDE algorithm showed the greatest improvement after optimization, with its CCDF curve significantly better than ABC and JADE in the high RSRP value region. When the CCDF value was 0.7, the RSRP value of PSO-MDE was about -75dBm, while ABC and JADE were about -90dBm and -85dBm, respectively. The reason for this result is related to the search strategy and adaptability. The PSO-MDE algorithm may have achieved a better balance between exploration and development, which can more effectively find solutions to improve RSRP during the optimization process.



4.3 Performance analysis of signal transmission power optimization algorithm based on MOPSO-DE

To verify the feasibility of the MOPSO-DE-based community signal optimization algorithm proposed in the study, a relatively new multi-objective optimization algorithm (Optimized Multi-Objective PSO, OMOPSO) and Non-dominated Sorting Genetic Algorithm III (NSGA-III) area selected for comparative experiments in terms of convergence speed and energy efficiency. The obtained results are shown in Figure 12.

Figures 12 (a) and (b) show the variation curves of fitness function values and system energy efficiency with iteration times for different algorithms, respectively. As shown in Figure 12 (a), MOPSO-DE algorithm reached a stable state after about 15 iterations, and the fitness function value was 0.15, while OMOPSO and NSGA-III were stable around 0.19 and 0.25 after 30 iterations, respectively. This fast convergence may be due to improvements in the MOPSO-DE algorithm, which makes it more efficient in the search process. As shown in Figure 12 (b), the energy efficiency of the MOPSO-DE algorithm continued to increase during the iteration process and stabilized after approximately 120 iterations, ultimately reaching about 5.4. In contrast, the energy efficiency of the OMOPSO algorithm fluctuated significantly during the iteration process, ultimately stabilizing at around 5.2, while the energy efficiency of the NSGA-III algorithm remained relatively stable throughout the entire iteration process, ultimately stabilizing at around 4.4. This indicates that the MOPSO-DE algorithm performs the best in improving system energy efficiency, possibly because it can better balance different objectives during the optimization process, thereby achieving higher energy efficiency. The experiment further explores the performance of various algorithms in signal transmission power optimization tasks, and the results are shown in Table 3.

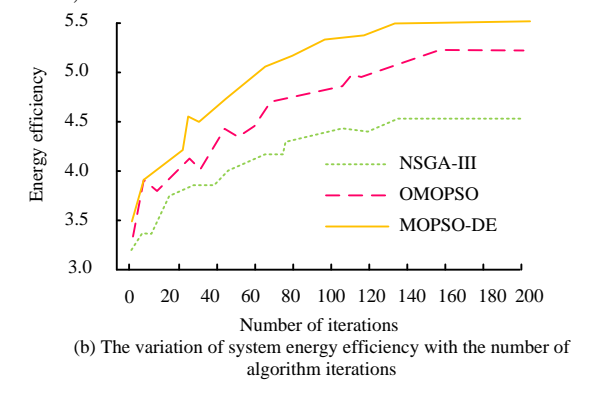


Figure 12: Performance variation curve of different algorithms with the number of iterations.

Algorithm	MOPSO-DE		OMOPSO		NSGA-III		SPEA2		PSO	
Iterations	100	200	100	200	100	200	100	200	100	200
Total transmission power (dBm)	35.2	33.5	36	34.5	37	35.5	36.8	36.0	35	35
Computation time(s)	110	530	120	550	100	540	130	520	100	500
Pareto front points	200	240	180	220	170	210	165	205	160	200
Standard deviation	0.5	0.3	0.7	0.6	0.4	0.2	0.5	0.5	0.6	0.6
p	p<0.01									

Table 3: Comparison results of signal transmission power optimization algorithm performance.

From Table 2, after 100 iterations, the performance of each optimization algorithm was significantly different in terms of signal transmission power control and Pareto solution quality. MOPSO-DE algorithm performed best with a minimum total transmission power of 35.2 DBM and 200 Pareto front points, and the standard deviation was 0.5, indicating that the algorithm had good stability in multiple operations. This is due to its fast convergence property that combines the global search capabilities of DE and PSO, which achieves an effective balance between exploration and utilization. The optimal transmission power of OMOPSO was 36.0 DBM, and the standard deviation was 0.7. The stability and energy efficiency of the solution were also good. The transmission power of NSGA-III was 37.0 DBM, which was the worst, but the standard deviation was 0.4, indicating that the algorithm was stable. It is speculated that it tends to maintain the diversity of solutions and sacrifice the convergence accuracy. Although the transmission power of traditional PSO was 35.0 DBM, which was close to MOPSO-DE, only 160 Pareto solutions were obtained, indicating that the distribution of solutions was insufficient and easy to fall into local optimum. In general, OMOPSO and MOPSO-DE are superior to the baseline algorithm in terms of convergence speed, solution set diversity, and power optimization, reflecting the enhanced role of subevolution mechanism in multi-objective problems. Statistical tests also showed that OMOPSO and MOPSO-DE had significant advantages (p<0.01).

5 Discussion

The proposed PSO-MDE and MOPSO-DE algorithms show significant performance advantages in antenna configuration and power allocation optimization of 5.5G cellular networks. By combining RT technology and PSO algorithm, these algorithms not only surpass the traditional PSO algorithm in convergence speed, but also show excellent performance in coverage gain and energy trade-off. PSO-MDE algorithm uses DE strategy to enhance the global search ability. The Metropolis criterion and adaptive inertia factor effectively avoid local optima, thereby accelerating convergence speed. This improvement makes the algorithm more balanced in global search and local fine adjustment in complex multi-

objective optimization problems. MOPSO-DE algorithm can significantly reduce energy consumption while ensuring network coverage by optimizing signal transmission power, which is of great significance to improve the energy efficiency and sustainability of the network.

Compared with the baseline algorithm, such as ABC, adaptive DE algorithm, OMOPSO, and NSGA-III, the proposed algorithm shows higher stability and consistency in coverage optimization and energy efficiency. When dealing with high-dimensional search space and nonlinear constraints, the baseline algorithm is often prone to fall into local optimization with slow convergence speed. It is difficult to balance different objectives in multi-objective optimization problems. In contrast, PSO-MDE and MOPSO-DE algorithms achieve better coverage and energy efficiency through accurate modeling and optimization strategies, providing an effective technical path for intelligent planning and performance improvement of 5.5G networks.

To sum up, the proposed algorithm shows obvious technical advantages in 5.5G network optimization, which not only improves the network coverage and energy efficiency, but also provides new ideas and methods for future network optimization. These achievements have important technical significance and application value for promoting the development of 5.5G and future communication technologies.

6 Conclusion

To improve the signal coverage performance and energy utilization efficiency of 5.5G cellular networks in the high frequency band, a joint optimization framework combining RTmodeling and multi-objective evolutionary algorithm was constructed to optimize antenna parameters and transmission power. The RT algorithm was taken to finely model the channel propagation characteristics in complex urban scenarios, and the optimization strategy was adopted to conduct multidimensional search and optimization on base stations in residential areas to maximize signal strength and minimize interference. In terms of antenna optimization, the optimal coverage of PSO-MDE algorithm was 0.645, which was 0.008 higher than JADE algorithm and 0.012 higher than ABC algorithm. The

average optimal coverage of PSO-MDE algorithm was 0.648, 0.009 higher than JADE algorithm and 0.015 higher than ABC algorithm. In terms of transmission power optimization, MOPSO-DE algorithm had the lowest total transmission power at 200 iterations, which was 33.5 DBM, 2.5 DBM lower than OMOPSO algorithm and 1.5 DBM lower than NSGA-III algorithm. The results show that the proposed joint optimization algorithm can effectively improve the performance of 5.5G network and provide an effective solution for network optimization. However, the research still has some limitations. Firstly, the experiment is based on static synthetic data, and the dynamic user behavior and time series channel changes have not been considered. In addition, the computational complexity of the algorithm used in large-scale, real-time optimization scenarios still needs to be further reduced. Therefore, future work will focus on the following directions. Firstly, online learning mechanism and dynamic adaptive strategies, such as adaptive PSO or reinforcement learning method, will be introduced to improve the real-time response ability of the model to environmental changes. Secondly, it combines the low complexity approximate optimization method to improve the deployment efficiency of the algorithm on edge devices. Thirdly, dynamic multi-user modeling and spatiotemporal channel data are integrated to enhance the generalization ability of the model to the real network environment. It is expected that these improvements will provide more practical and forwardlooking technical support for intelligent optimization of 5.5G and even future 6G networks.

Reference

- [1] Zhi Liu, and Wei Song. Search guidance network assisted dynamic particle swarm optimization algorithm. Journal of Frontiers of Computer Science and Technology, 18(12):3189-3202, 2024.https://doi.org/10.3778/j.issn.1673-9418.2312030
- [2] Dan Song, Zhiping Xu, Shaohua Hong, and Lin Wang. Survey of transmission coding theory on physical layer for wireless body area network: optimal design of low-density parity-check code. Journal of Electronics & Information Technology, 45(08):2818-2827,
 - 2023.https://doi.org/10.11999/JEIT221171
- [3] Baohui Han, Qichao Zhao, Rong Chang, Xiaomeng Li, Keqin Yan, and Qiming Fu. Chlorophyll-a concentration inversion model: stacked autoencoder particle swarm optimization BP neural network. Journal of Geo-Information Science, 25(09):1882-1893,
- 2023.https://doi.org/10.12082/dqxxkx.2023.230144
 [4] Zhisheng Niu. uRLLC3: ultra-reliable and low-latency communication, computing, and control for 6G networks. Scientia Sinica Informationis, 54(05):1267-1282,
 - 2024.https://doi.org/10.1360/SSI-2023-0336

- [5] Yi He, Weizhi Zhong, Shiqing Wan, Qiuming Zhu, and Zhipeng Lin. Joint beamforming for IRS-aided MU-MISO millimeter wave communication of vehicular network. Journal of Signal Processing, 40(02):336-344, 2024.https://doi.org/10.16798/j.issn.1003-0530.2024.02.011
- [6] Li Juan. Improved genetic algorithm enhanced with generative adversarial networks for logistics distribution path optimization. Informatica, 49(11):180-197,
 - 2025.https://doi.org/10.31449/inf.v49i11.6961
- [7] Chenxi Mao, Yongchao Guo, Haoyu Zhang, and Liangquan Zhang. Post-earthquake damage assessment for RC frame communication buildings based on convolutional neural network. Journal of Natural Disasters, 33(05):157-167, 2024.https://doi.org/10.13577/j.jnd.2024.0515
- [8] Wenwu Yu, Xiaokai Nie, Yujin Cai, Guangju Li, Hongzhe Liu, Qiang Cheng, and Tiejun Cui. A survey on the performance optimization of wireless communication networks assisted by reconfigurable intelligent surface. Scientia Sinica Informationis, 54(11):2503-2517, 2024.https://doi.org/10.1360/SSI-2024-0060
- [9] Chen Liang, Deqiang He, Ziyang Ren, Zhenzhen Jin, and Weifeng Yang. Real-time traffic scheduling optimization of train communication network based on time-sensitive network. Journal of Railway Science and Engineering, 21(01):58-69, 2024.https://doi.org/10.19713/j.cnki.43-1423/u.T20230194
- [10] Kaiwen Yu, Renhe Fan, Wenlong Gou, Chuanhang Yu, and Gang Wu. Cross-layer energy efficiency optimization for semantic communication networks. Scientia Sinica Informationis, 54(04):758-776, 2024.https://doi.org/10.1360/SSI-2023-0283
- [11] Wenzhuo Hu, and Chun Wu. A hierarchical genetic algorithm for spatio-temporal coverage optimization in communication networks under emergency monitoring scenarios. Journal of Geo-Information Science, 26(08):1880-1892, 2024.https://doi.org/10.12082/dqxxkx.2024.230732
- [12] Yurong Wang, Weiwei Qu, Guilin Li, Hu Deng, and Liping Shang. An optimization method for terahertz metamaterial absorber based on multi-objective particle swarm optimization. Acta Physica Sinica, 74(05):057801, 2025.https://doi.org/10.7498/aps.74.20241684
- [13] Praveena Nuthakki, Pavan Kumar T, Musaed Alhussein, Muhammad Shahid Anwar, Khursheed Aurangzeb, Leenendra Chowdary Gunnam. Aldriven resource and communication-aware virtual machine placement using multi-objective swarm optimization for enhanced efficiency in cloud-based smart manufacturing. Computers, Materials & Continua, 81(12):4743-4756, 2024.https://doi.org/10.32604/cmc.2024.058266
- [14] Hongwei Zhao, Yongfang Xie, Jianhua Liu, Jiayi Hou, and Haichao Liu. Research on deployment optimization strategy and application technology of

- 5G high-speed rail network. Railway Standard Design, 67(01):167-174, 2023.https://doi.org/10.13238/j.issn.1004-2954.202111180005
- [15] Yifan Zhang, and Wei Song. Multi-objective particle swarm optimization algorithm guided by extreme learning decision network. Journal of Frontiers of Computer Science and Technology, 18(06):1513-1525, 2024.https://doi.org/10.3778/j.issn.1673-9418.2304026
- [16] Hao Li, Haixiao Yang, Lan Zhang, Xin Huang, Haining Wang, and Yan Kang. Improved discrete mayfly algorithm for multi-objective dynamic network community detection. Journal of Frontiers of Computer Science and Technology, 17(04):942-952, 2023.https://doi.org/10.3778/j.issn.1673-9418.2106011
- [17] Yifei Zou, Senmao Qi, Cong'an Xu, and Dongxiao Yu. Distributed weighted data aggregation algorithm in end-to-edge communication networks based on multi-armed bandit. Computer Science, 50(02):13-22,
- 2023.https://doi.org/10.11896/jsjkx.221100134
 [18] Junhai Zhao, Linwei Hua, and Yu Wang. Study on axial compressive load bearing capacity of concrete-filled double-skin steel tubular columns based on particle swarm optimization BP neural network. Progress in Steel Building Structures, 26(09):

 45-52,

2024.https://doi.org/10.13969/j.cnki.cn31-1893.2024.09.005

- [19] Na Luo, Hua Yu, Zeqing You, Yao Li, Tunan Zhou, Nan Han, Chenxu Liu, Zihan Jiang, and Shaojie Qiao. Fuzzy logic and neural network-based risk assessment model for import and export enterprises: a review. Journal of Data Science and Intelligent Systems, 1(1): 2-11, 2023.https://doi.org/10.47852/bonviewJDSIS32021 078
- [20] Xingyu Sha, Jiaqi Zhang, and Keyou You. Fully asynchronous distributed optimization with linear convergence over directed networks. Journal of Sun Yat-sen University (Natural Science Edition), 62(05): 1-23, 2023.https://doi.org/10.13471/j.cnki.acta.snus.2023 A023
- [21] Chunlei Zhong, and Gang Yang. Design and application of improved genetic algorithm for optimizing the location of computer network nodes. Informatica, 49(16):25-51, 2025.https://doi.org/10.31449/inf.v49i16.7201
- [22] Yan Yang, and Kang Wang. Efficient logistics path optimization and scheduling using deep reinforcement learning and convolutional neural networks. Informatica, 49(16):43-59, 2025.https://doi.org/10.31449/inf.v49i16.7839
- [23] Mikel Barbara, David Rey, Taha Rashidi, and Divya Nair. School choice modeling and network optimization in an urban environment. Annals of

- Regional Science, 72(3):115-131, 2024.https://doi.org/10.1007/s00168-023-01230-5
- [24] Greanne Leeftink, Kimberley Morris, Tim Antonius, Willem de Vries, and Erwin Hans. Interorganizational pooling of NICU nurses in the Dutch neonatal network: a simulation-optimization study. Health Care Management Science, 28(1):64-83, 2025.https://doi.org/10.1007/s10729-025-09697-8